

October 27, 2018

hep-ph/01xxx

# Heavy quark polarizations of $e^+e^- \rightarrow q\bar{q}h$ in the general two Higgs doublet model

CHAO-SHANG HUANG <sup>a</sup>, SHOU-HUA ZHU<sup>b</sup>

<sup>a</sup> *Institute of Theoretical Physics, Academia Sinica,  
P.O.Box 2735, Beijing 100080, P.R.China*

<sup>b</sup> *Institut für Theoretische Physik, Universität Karlsruhe,  
D-76128 Karlsruhe, Germany*

The polarizations of the heavy quark ( $q = t$  or  $b$ ) in the process  $e^+e^- \rightarrow q\bar{q}h$  have been calculated in the general two Higgs doublet model. The CP violating normal polarization of the top quark can reach 8%, and  $2 \sim 3\%$  for the bottom quark, while it is zero in the standard model. The longitudinal and transverse polarizations of the bottom quark can be significantly different from those in SM and consequently could also be used as the probe of the new physics.

Searching for a Higgs boson has been a major motivation for many current and future collider experiments, since Higgs bosons encode the underlying physics of mass generation. The Next Linear Collider (NLC) running at center-of-mass (CMS) energies from 0.5 to 2 TeV is designed to examine the nature of the Higgs bosons in detail. The present lower bounds on Higgs boson mass from the direct searches are  $m_h > 114.1$  GeV (at 95% CL) [1] for the standard model (SM) Higgs boson, and  $m_h > 91.0$  GeV and  $m_A > 91.9$  GeV (at 95% CL) [2] for the light neutral scalar and pseudoscalar Higgs bosons of the minimal supersymmetric standard model (MSSM). In the MSSM the upper bound of the light neutral scalar Higgs boson mass is predicted to be about 130 GeV [3]. Therefore, it is possible and expected to examine the properties of the Higgs bosons in the process  $e^+e^- \rightarrow q\bar{q}h$  ( $q=t, b$ ) at NLC.

It has been estimated that a detailed investigation of cross-sections of a few fb is possible at NLC with a yearly integrated luminosity of the order of  $100 \text{ fb}^{-1}$  [4]. The associated production of a Higgs boson with a pair of heavy fermion-antifermion is of a good place to study the couplings of Higgs bosons to fermions, in particular, to probe new Higgs-fermion interactions at the tree level. The possibility of observing large signatures of new CP-violating and flavor-changing Higgs-quark couplings in NLC experiments has been discussed [5].

If there are CP violating couplings in the extended Higgs sector (e.g., in a general two Higgs model, MSSM etc.) CP violation in the process  $e^+e^- \rightarrow q\bar{q}h$  arises because of interference of the diagrams where the Higgs bosons is coupled to a Z boson with the diagrams where the Higgs boson is radiated off the quark or anti-quark. There are two kinds of CP-odd observables that can trace the tree level CP effects in the process  $e^+e^- \rightarrow q\bar{q}h$ . One is consisted of the triple momenta  $\mathbf{O} = \vec{p}_- \cdot (\vec{p}_q \times \vec{p}_{\bar{q}})$ , the other is of the mixed triplet of momenta and spin  $P_N = \vec{s}_q \cdot (\vec{p}_- \times \vec{p}_q)$ , i.e., the normal polarization of the quark. The formmer is examined in  $e^+e^- \rightarrow t\bar{t}h$  in ref. [5], and we shall study the latter in the paper. It is known that in the semi-leptonic decay  $B \rightarrow X_s l^+ l^-$ ,  $P_N$  is the CP-violating projection of the lepton spin onto the normal of the decay plane. Because  $P_N$  in  $B \rightarrow X_s l^+ l^-$  comes from both the quark and lepton sectors, purely hadronic and leptonic CP-violating observables, such as  $d_n$  or  $d_e$ , do not necessarily strongly constrain  $P_N$  [6]. So it is advantageous to use  $P_N$  to investigate CP violation effects in some extensions of SM [7]. For  $e^+e^- \rightarrow q\bar{q}h$ ,  $P_N$  can be defined as the CP-violating projection of the quark spin onto the normal of the plane determined by  $\vec{p}_{e^-}$  and

$\vec{p}_q$ . Although there is no advantage mentioned above, it is useful to investigate CP effects by measuring  $P_N$  since it can give more information on the couplings of Higgs to fermions. We find that the normal polarization  $P_N$  of the heavy quark in  $e^+e^- \rightarrow q\bar{q}h$  is sensitive to CP violation effects due to the extended Higgs sector. Therefore, the two kinds of CP-odd observables are complementary each other in probing the CP-odd couplings of Higgs bosons to quarks. In the paper we shall investigate the polarizations of  $q$  ( $q=t, b$ ) and the cross section for the  $q\bar{q}h$  production at NLC in a general two-Higgs-doublet model.

In the general two-Higgs-doublet model used here [8], the  $hq\bar{q}$  interaction lagrangian piece ( $h$  represents one of the three neutral Higgs boson) can be written as:

$$\mathcal{L} = -\frac{g_W}{2m_W} \left( m_t h \bar{t}(a_t + ib_t \gamma_5)t + m_b h \bar{b}(a_b + ib_b \gamma_5)b \right). \quad (1)$$

If we choose  $h = H_1$  as Ref. [8],  $a$  and  $b$  can be expressed as

$$\begin{aligned} a_t; a_b &= \frac{\cos \alpha_1}{\sin \beta}; \quad -\frac{\sin \alpha_1 \cos \alpha_2}{\cos \beta}, \\ b_t; b_b &= \cot \beta \sin \alpha_1 \sin \alpha_2; \quad \tan \beta \sin \alpha_1 \sin \alpha_2 \end{aligned} \quad (2)$$

with  $\tan \beta \equiv v_u/v_d$  and  $v_u(v_d)$  is the vacuum-expectation-value (VEV) responsible for giving mass to the up(down) quark. Three Euler angles  $\alpha_{1,2,3}$  [8] parameterize the neutral Higgs mixing matrix. Note that in the SM, the only couplings of the one neutral Higgs present, and  $a_{t,b}^h = 1, b_{t,b}^h = 0$ .

For the process  $e^+(p_2)e^-(p_1) \rightarrow h(k_1)t(k_2)\bar{t}(k_3)^*$ , we define  $(p_1 + p_2)^2 = S$ . And the amplitude is as following

$$\begin{aligned} M = \frac{e^3}{4c_w^4 s_w^3 m_w} \{ & \bar{u}(k_2)\gamma_\mu(f_1 P_R + f_2 P_L)v(k_3)\bar{v}(p_2)\gamma_\mu P_R u(p_1) + \bar{u}(k_2)\gamma_\mu(f_3 P_R \\ & + f_4 P_L)v(k_3)\bar{v}(p_2)\gamma_\mu P_L u(p_1) + c_w^2 m_t [\bar{u}(k_2)(f_5 P_R + f_6 P_L)v(k_3)\bar{v}(p_2) \not{k}_2 P_R u(p_1) + \bar{u}(k_2)(f_7 P_R \\ & + f_8 P_L)v(k_3)\bar{v}(p_2) \not{k}_2 P_L u(p_1) + \bar{u}(k_2)(f_9 P_R + f_{10} P_L)v(k_3)\bar{v}(p_2) \not{k}_3 P_R u(p_1) + \bar{u}(k_2)(f_{11} P_R \\ & + f_{12} P_L)v(k_3)\bar{v}(p_2) \not{k}_3 P_L u(p_1) + \frac{1}{2}(\bar{u}(k_2)(\not{p}_1 + \not{p}_2)\gamma_\mu P_R v(k_3)\bar{v}(p_2)\gamma_\mu(f_{13} P_R + f_{14} P_L)u(p_1) \\ & + \bar{u}(k_2)(\not{p}_1 + \not{p}_2)\gamma_\mu P_L v(k_3)\bar{v}(p_2)\gamma_\mu(f_{15} P_R + f_{16} P_L)u(p_1))] \}, \end{aligned} \quad (3)$$

---

\*For the simplicity of presentation, we give the formulas for  $t\bar{t}h$  production. The results of  $b\bar{b}h$  production could be easily obtained by substituting the couplings and kinematic variables.

where

$$f_1 = (-g_A^e + g_V^e) \left( -F_2 A c_w^2 g_A^t m_t^2 - F_4 A^* c_w^2 g_A^t m_t^2 + F_5 (g_V^t - g_A^t) c m_w^2 \right), \quad (4)$$

$f_2$  is obtained by substituting  $-g_A^t$  for  $g_A^t$  and  $A^*$  for  $A$  in  $f_1$ ,  $f_3$  by substituting  $-g_A^e$  for  $g_A^e$  in  $f_1$ , and  $f_4$  by substituting  $-g_A^t$  for  $g_A^t$ ,  $A^*$  for  $A$  and  $-g_A^e$  for  $g_A^e$  in  $f_1$ ,

$$f_5 = F_2 A (g_A^t + g_V^t) (g_V^e - g_A^e) + F_5 c \eta (g_V^e - g_A^e) + 4 F_1 A c_w^2 e_t s_w^2 \quad (5)$$

$f_6$  is obtained by substituting  $-g_A^t$  for  $g_A^t$  and  $A^*$  for  $A$  in  $f_5$ ,  $f_7$  by substituting  $-g_A^e$  for  $g_A^e$  in  $f_5$ , and  $f_8$  by substituting  $-g_A^t$  for  $g_A^t$ ,  $A^*$  for  $A$  and  $-g_A^e$  for  $g_A^e$  in  $f_5$ ,

$$f_9 = F_4 A (g_A^t - g_V^t) (g_V^e - g_A^e) + F_5 c \eta (g_V^e - g_A^e) - 4 F_3 A c_w^2 e_t s_w^2 \quad (6)$$

$f_{10}$  is obtained by substituting  $-g_A^t$  for  $g_A^t$  and  $A^*$  for  $A$  in  $f_9$ ,  $f_{11}$  by substituting  $-g_A^e$  for  $g_A^e$  in  $f_9$ , and  $f_{12}$  by substituting  $-g_A^t$  for  $g_A^t$ ,  $A^*$  for  $A$  and  $-g_A^e$  for  $g_A^e$  in  $f_9$ ,

$$f_{13} = A \left( (g_V^e - g_A^e) [F_2 (g_V^t + g_A^t) + F_4 (g_V^t - g_A^t)] + 4 (F_1 + F_3) c_w^2 e_t s_w^2 \right) \quad (7)$$

$f_{14}$  is obtained by substituting  $-g_A^e$  for  $g_A^e$  in  $f_{13}$ ,  $f_{15}$  by substituting  $-g_A^t$  for  $g_A^t$  and  $A^*$  for  $A$  in  $f_{13}$ ,  $f_{16}$  by substituting  $-g_A^t$  for  $g_A^t$ ,  $A^*$  for  $A$  and  $-g_A^e$  for  $g_A^e$  in  $f_{13}$ ,

$$A = a + ib, \quad (8)$$

$$\frac{1}{F_1} = S (S - 2k_2 \cdot (p_1 + p_2)), \quad (9)$$

$$\frac{1}{F_2} = (S - m_z^2) (S - 2k_2 \cdot (p_1 + p_2)), \quad (10)$$

$1/F_3$  and  $1/F_4$  are obtained by substituting  $k_3$  for  $k_2$  in  $1/F_1$  and  $1/F_2$  respectively,

$$\frac{1}{F_5} = (S - m_z^2) (2k_2 \cdot k_3 + 2m_t^2 - m_z^2). \quad (11)$$

In above equations,  $c$  is the coupling constant of  $z^0 - z^0 - h$  ( $c = 1$  corresponding to the SM case [8])

$$c = \sin \beta \cos \alpha_1 + \cos \beta \sin \alpha_1 \cos \alpha_3, \quad (12)$$

$g_A^e = 1/2$ ,  $g_V^e = 1/2 - 2s_w^2$ ,  $g_A^t = 1/2$ ,  $g_V^t = 1/2 - 4/3s_w^2$ ,  $e_t$  is the top quark charge, for top quark  $\eta = 1$  and for bottom  $\eta = -1$ .

The next step is to square the amplitude while keeping top quark spin information. Technically, we use  $u\bar{u} = \frac{1}{2}(\not{p} + m)(1 + \lambda\not{s}\gamma_5)$ , where  $s$  is the lorentz spin vector and  $\lambda = \pm 1$ . Because expressions are lengthy, we don't show it here explicitly. Let us now discuss the quark polarization effects. We define three orthogonal unit vectors:

$$\begin{aligned}\vec{e}_L &= \frac{\vec{p}_t}{|\vec{p}_t|}, \\ \vec{e}_N &= \frac{\vec{p}_{e^-} \times \vec{p}_t}{|\vec{p}_{e^-} \times \vec{p}_t|}, \\ \vec{e}_T &= \vec{e}_N \times \vec{e}_L,\end{aligned}$$

where  $\vec{p}_{e^-}$  and  $\vec{p}_t$  are the three momenta of the  $e^-$  and the  $t$  quark, respectively, in the center of mass of the  $e^+ e^-$  system.  $P_L$ ,  $P_T$ , and  $P_N$ , which correspond to the longitudinal, transverse and normal projections of the top spin, respectively, are defined as

$$P_i(s) = \frac{\sigma(\vec{n} = \vec{e}_i) - \sigma(\vec{n} = -\vec{e}_i)}{\sigma(\vec{n} = \vec{e}_i) + \sigma(\vec{n} = -\vec{e}_i)}. \quad (13)$$

In our numerical examples, we choose the  $h$  as the lightest mass Higgs and ignore other neutral Higgs contributions. Because we are mainly interested in the CP violation effects for the process, as a numerical example, the mixing angles are taken as  $\alpha_1 = \alpha_2 = \pi/4$  and  $\alpha_3 = 0$ .

In Fig. 1-3, the top quark polarizations and cross sections are presented as function of the Higgs boson mass, CMS energy and  $\tan\beta$ . The cross sections for  $t\bar{t}h$  have been given [5] and our results are in agreement with the previous ones. We see from the figures that the  $P_N$  can reach  $\sim 8\%$  and decreases with the increase of  $\tan\beta$ , while  $P_N$  is equal to zero in the SM. On the contrary, the longitudinal and transverse polarizations in the 2HDM don't change much compared to those in the SM, if the Higgs mass in the 2HDM is equal to that in SM.

In Fig. 4-6, the bottom quark polarizations and cross sections are presented as function of the Higgs boson mass, CMS energy and  $\tan\beta$ . We can see that the  $P_N$  increases with the increment of  $\tan\beta$  and can reach  $2 \sim 3\%$ . The longitudinal and transverse polarizations in the 2HDM can differ a lot compared to those in the SM.

We would like to discuss the statistic significance in measuring the CP violating observable  $P_N$  with emphasis on estimating the sensitivity to  $\tan\beta$ . The statistic significance is defined

by [5]  $N_{SD} = P_N \sqrt{L} \sqrt{\sigma}$ , where  $L$  is the effective luminosity for fully reconstructed  $q\bar{q}h$  events and  $\sigma$  is the production cross section for  $e^+e^- \rightarrow q\bar{q}h$ . We take  $L = \epsilon \mathcal{L}$ , where  $\mathcal{L}$  is the total yearly integrated luminosity and  $\epsilon$  is the overall efficiency for reconstruction of the  $q\bar{q}h$  final state. For illustrative purposes, we choose  $\mathcal{L} = 200 fb^{-1}$ ,  $\epsilon = 0.5$  (if  $\epsilon = 0.25$  our results would correspondingly require 2 years of running),  $m_h = 150$  GeV and other model parameters same as those in Fig. 3. For  $q=t$ ,  $P_N$  can be observed at a  $1\sigma$  level (which corresponds to  $N_{SD}/\sqrt{L} = 0.1$ ) for  $\tan\beta \sim 0.6$  and at a  $6.5\sigma$  level for  $\tan\beta = 0.1$ . For  $q=b$ , taking the values of the parameters as in Fig. 6, even for  $\tan\beta = 50$ ,  $L = 2000 fb^{-1}$  is needed in order to observe  $P_N$  at a  $1\sigma$  level.

To summarize, the polarizations of the heavy quark ( $t$  and  $b$ ) of the process  $e^+e^- \rightarrow q\bar{q}h$  have been calculated in the general two Higgs doublet model. We should note here that even for MSSM, the sizable Higgs sector CP violation can be induced at one-loop, which can manifest themselves in the couplings of the lightest neutral Higgs boson to the SM fermions [9]. Our numerical results show that the normal polarization of the top quark can reach 8%, and  $2 \sim 3\%$  for bottom quark, which are zero in the SM. At the same time, the longitudinal and transverse polarizations of the bottom quark can be significantly different from those in SM and consequently could also be used as the probe of the new physics for the process  $e^+e^- \rightarrow b\bar{b}h$ . As it is well-known, the top quark decays as a free quark since its lifetime is so short that it has no time to bind with light quarks before it decays. Therefore, the top quark polarizations can be measured by measuring the energy spectra of its decay W's, or of leptons from W decays [10]. Furthermore, a linear collider with  $200 fb^{-1}$  will begin to be sensitive to  $\tan\beta < 0.6$ , for the  $t\bar{t}h$  final state if the Higgs boson  $h$  is light (say, smaller than or equal to 150 GeV) and the mixing angles of neutral Higgs bosons are not close to the end points 0 and  $\pi/2$ . For  $b$  quark, its polarizations can be measured by measuring those of its fragmentation  $\Lambda_b$ . Nevertheless, it is not easy to observe due to the small probability (the probability that a bottom quark fragmentizes into a  $\Lambda_b$  is about 10 %).

The author would like to thank G. Eilam and S. Bar-Shalom for useful discussions. This work was supported in part by the Alexander von Humboldt Foundation and National Nature Science Foundation of China.

- 
- [1] LHWG Note/2001-03, CERN-EP/2001-055, July 2001.
- [2] LHWG Note/2001-04, July 2001.
- [3] S. Heinemeyer, W. Hollik and G. Weiglein, Eur. Phys. J. C **9**, 343 (1999) [arXiv:hep-ph/9812472].
- [4] For example to see, J. A. Aguilar-Saavedra *et al.* [ECFA/DESY LC Physics Working Group Collaboration], arXiv:hep-ph/0106315.
- [5] J.F. Gunion, B. Grzadkowski and X.-G. He, Phys. Rev. Lett. **77** (1996)5172; J.F. Gunion and X.-G. He, hep-ph/9709453; S. Bar-Shalom, arXiv:hep-ph/9710355; S. Bar-Shalom, D. Atwood, G. Eilam, R. R. Mendel and A. Soni, Phys. Rev. D **53**, 1162 (1996) [arXiv:hep-ph/9508314]; D. Atwood, S. Bar-Shalom, G. Eilam and A. Soni, Phys. Rept. **347**, 1 (2001) [arXiv:hep-ph/0006032]; M. Spira, hep-ph/0101314 and references therein.
- [6] R. Garisto, Phys. Rev. **D51** (1995) 1107.
- [7] R. Garisto and G. Kane, Phys. Rev. **D44** (1991) 2038.
- [8] C.D. Froggat, R.G. Moorhouse and I.G. Knowles, Nucl. Phys. **B386** 63 (1992); W. Bernreuther, T. Schröder and T.N. Pham, Phys. Lett. **B279**, 389 (1992).
- [9] See for example, K. S. Babu, C. Kolda, J. March-Russell and F. Wilczek, Phys. Rev. D **59**, 016004 (1999) [arXiv:hep-ph/9804355].
- [10] C.R. Schmidt and M.E. Peskin, Phys. Rev. Lett. **69** (1992) 410; G.L. Kane, G.A. Ladinsky and C.-P. Yuan, Phys. Rev. **D45** (1992) 124.

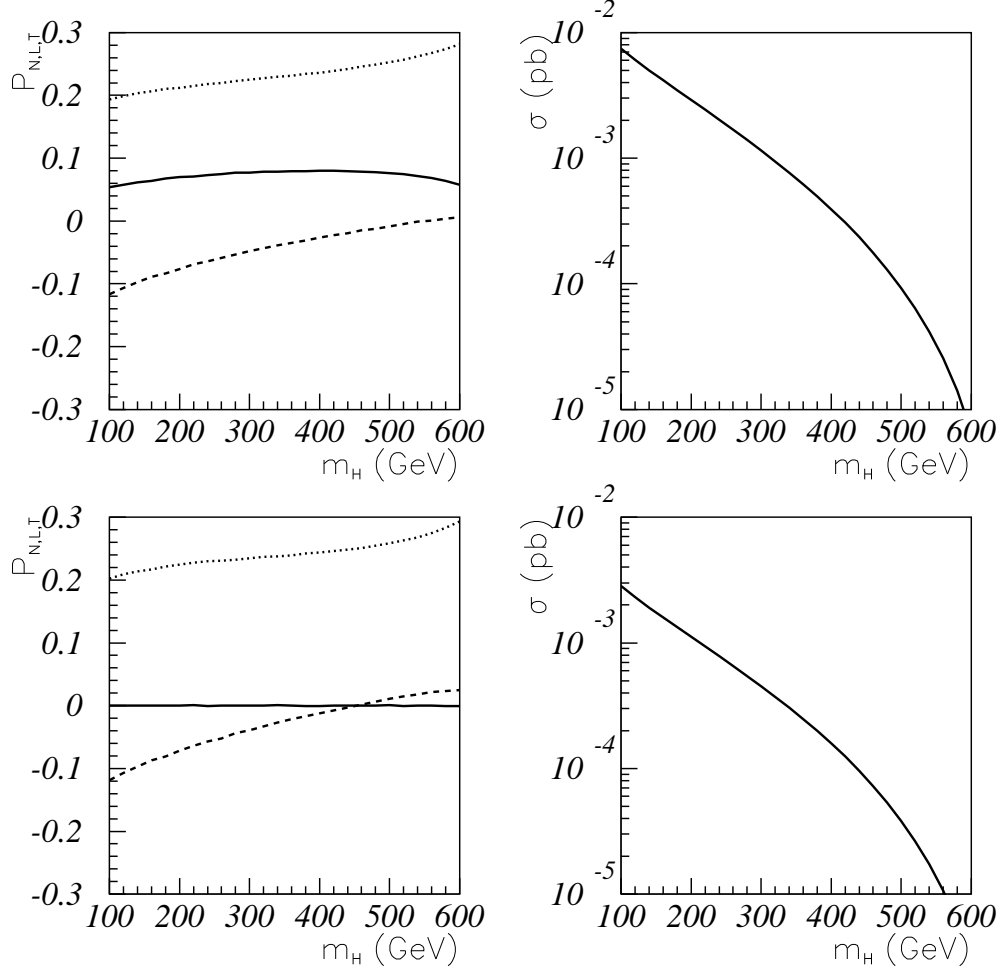


FIG. 1. Polarizations of top quark and the cross section as function of Higgs mass for  $e^+e^- \rightarrow t\bar{t}h$ , where  $\sqrt{s} = 1$  TeV, the upper two figures represent those in 2HDM and the lower in SM. The solid, dashed and dot-dashed lines represent the normal, longitudinal and transverse polarization of the top quark respectively, and for 2HDM, parameters are  $\tan\beta = 0.5$ ,  $\alpha_1 = \pi/4$ ,  $\alpha_2 = \pi/4$ ,  $\alpha_3 = 0$ .



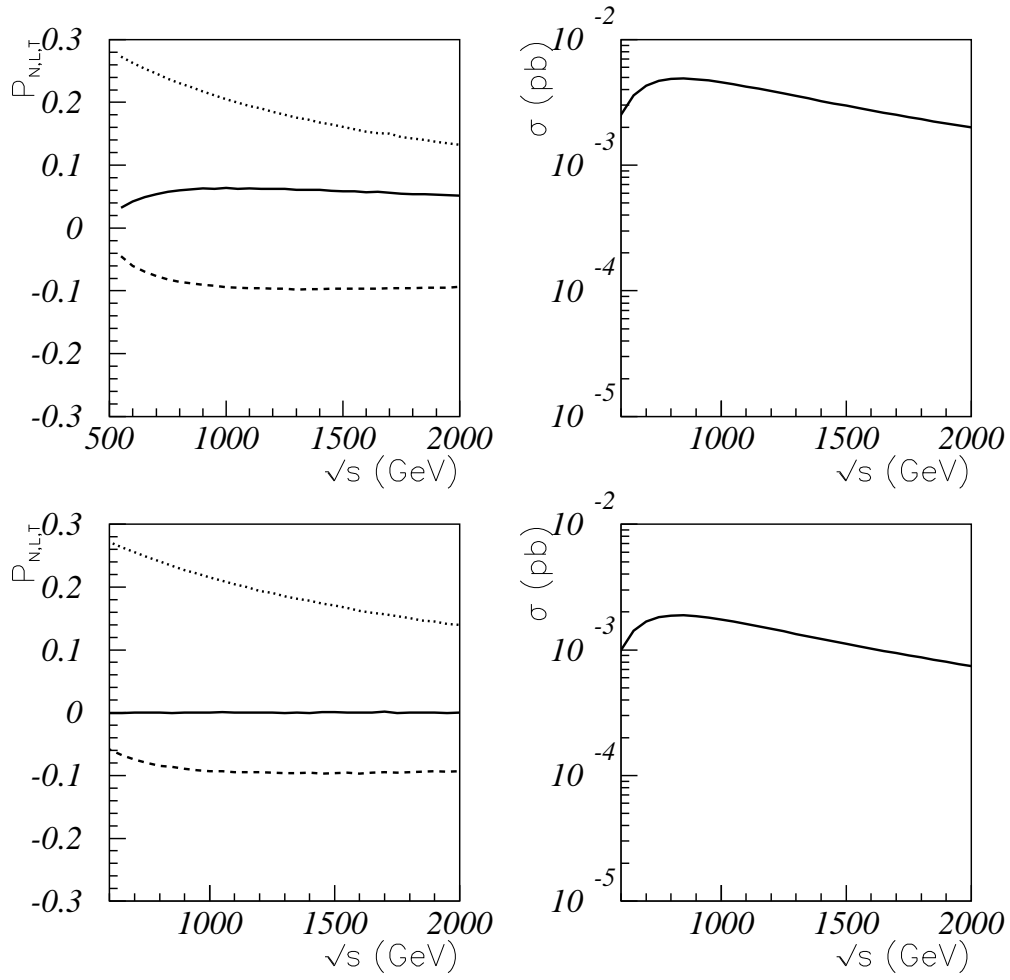


FIG. 2. Polarizations of top quark and the cross section as function of center-of-mass-energy of  $e^+e^-$  for  $e^+e^- \rightarrow t\bar{t}h$ , where  $m_h = 150$  GeV. Other parameters and captions are same as Fig. 1.

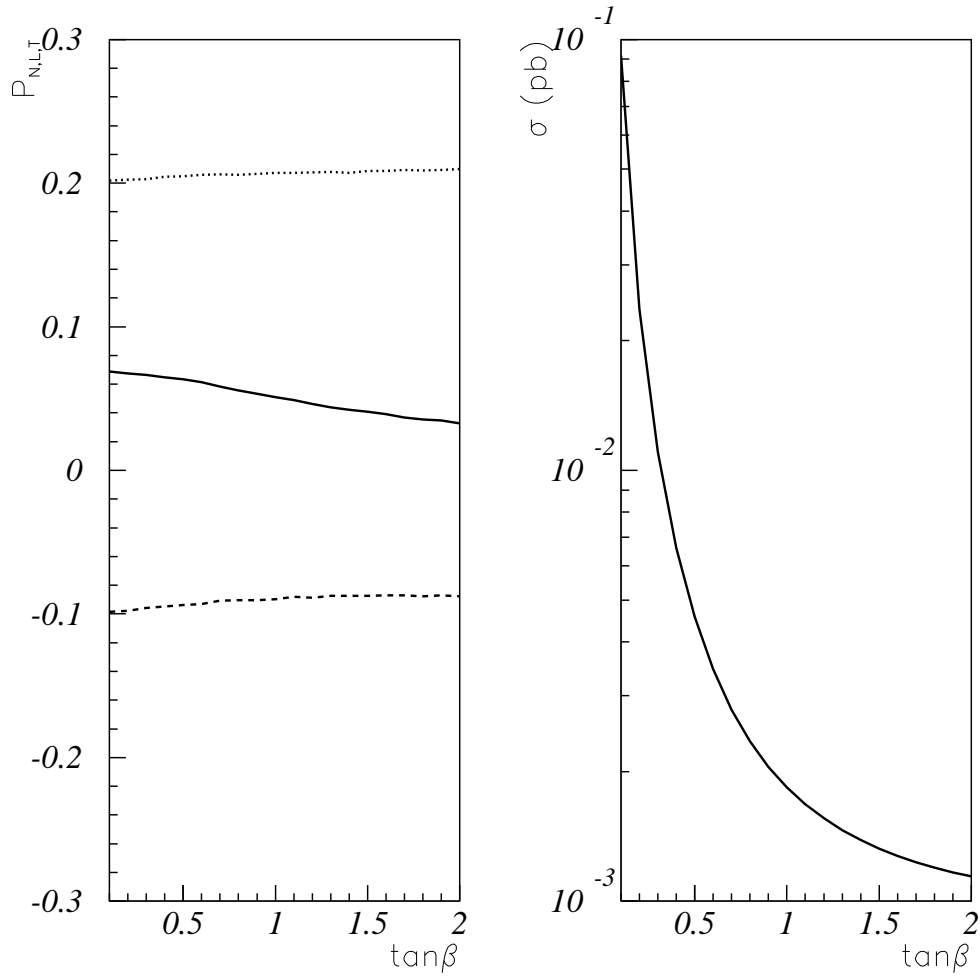


FIG. 3. Polarizations of top quark and the cross section as function of  $\tan\beta$  for  $e^+e^- \rightarrow t\bar{t}h$ , where center-of-mass-energy of  $e^+e^-$  is 1 TeV and  $m_h = 150$  GeV. Other model parameters are same as Fig.

1.

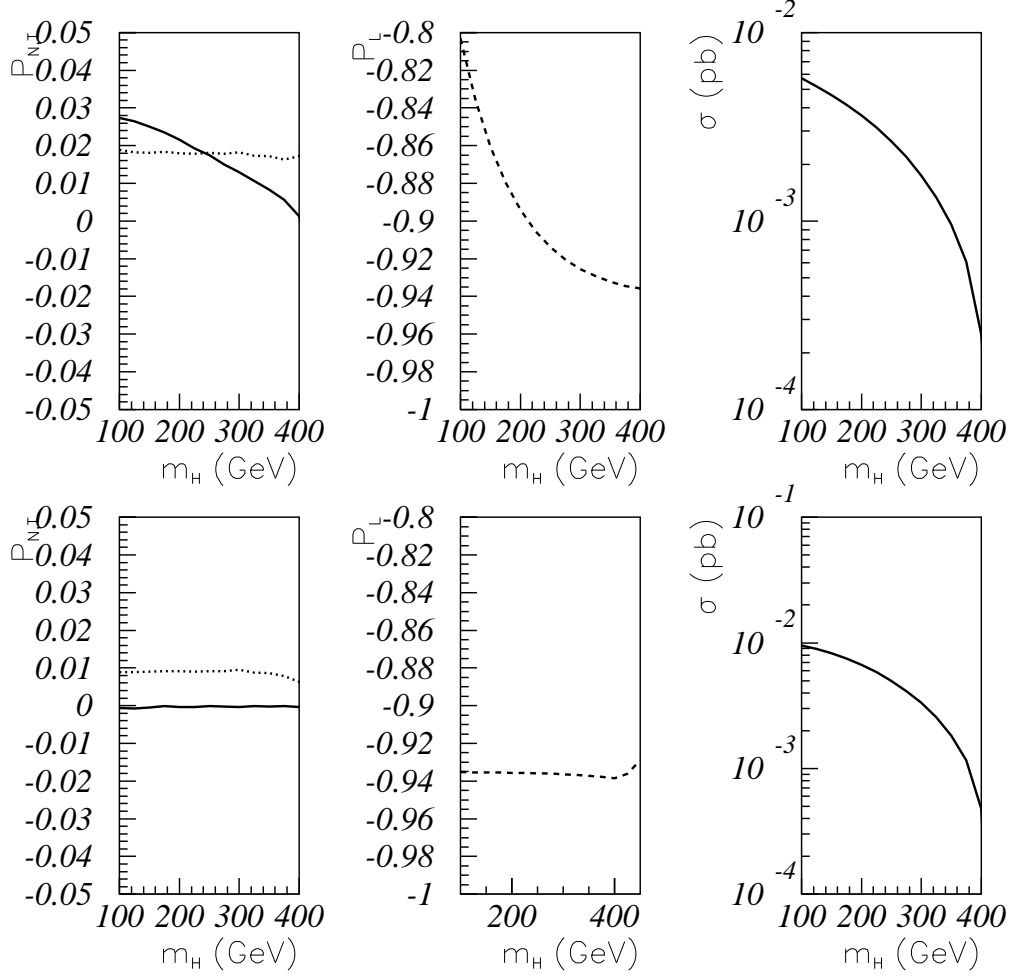


FIG. 4. Polarizations of bottom quark and the cross section as function of Higgs mass for  $e^+e^- \rightarrow b\bar{b}h$ , where  $\sqrt{s} = 0.5$  TeV, the upper three figures represent those in 2HDM and the lower in SM. For 2HDM, parameters are  $\tan\beta = 50$ ,  $\alpha_1 = \pi/4$ ,  $\alpha_2 = \pi/4$ ,  $\alpha_3 = 0$ , and for left column, solid and dashed lines represent the normal and transverse polarization of the bottom quark respectively.

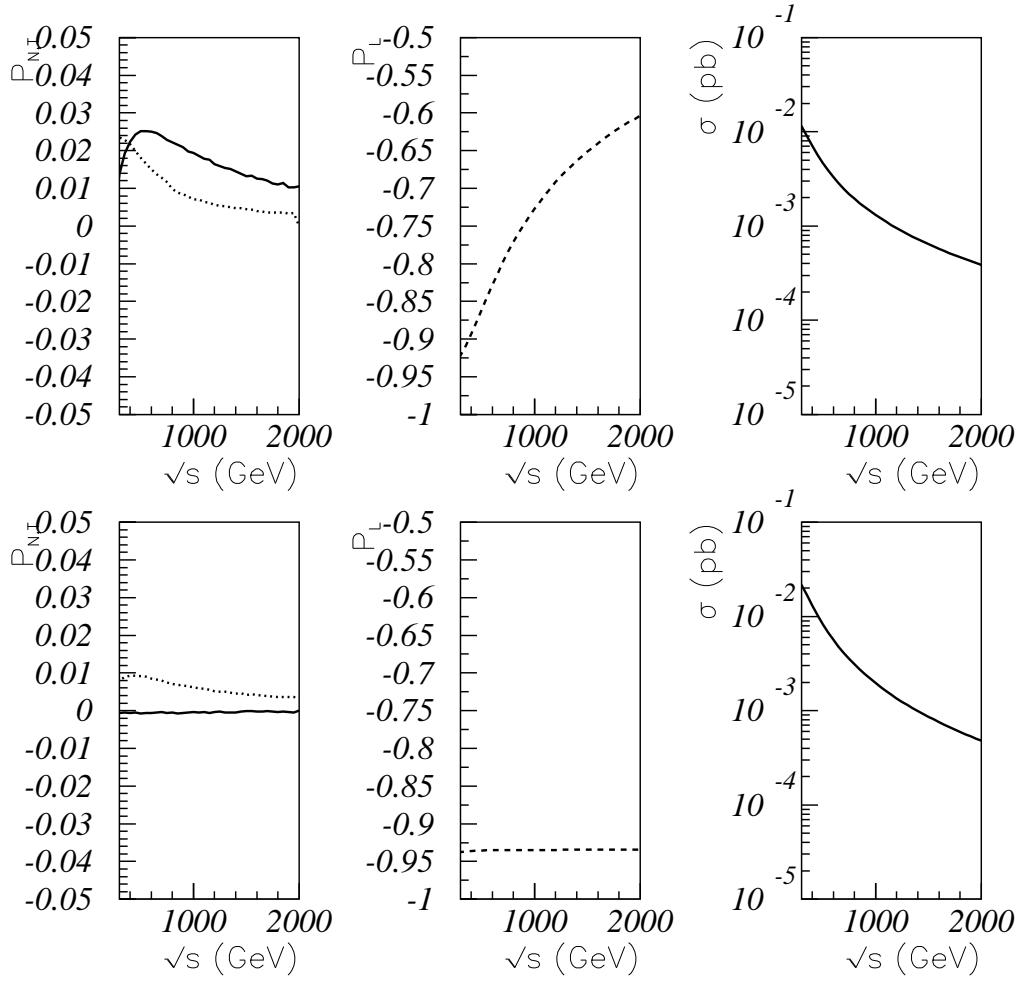


FIG. 5. Polarizations of bottom quark and the cross section as function of center-of-mass-energy of  $e^+e^-$  for  $e^+e^- \rightarrow b\bar{b}h$ , where  $m_h = 150$  GeV. Other parameters and captions are same as Fig. 4.

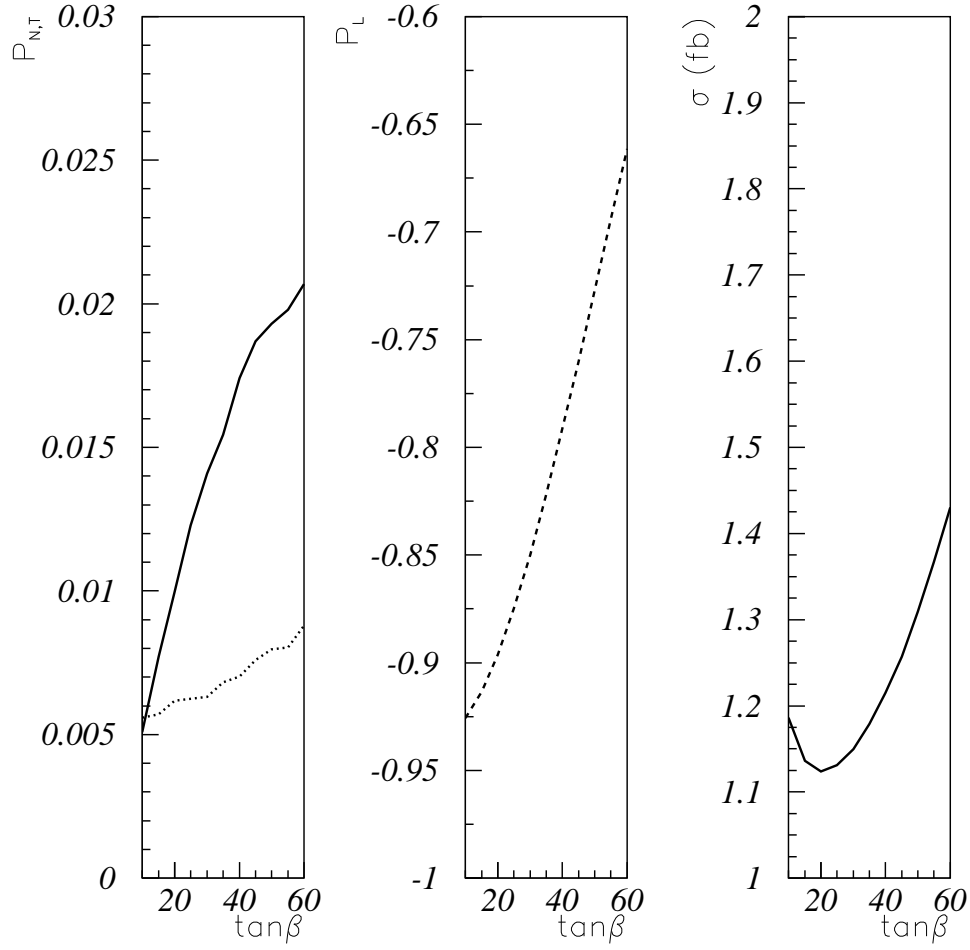


FIG. 6. Polarizations of bottom quark and the cross section as function of  $\tan\beta$  for  $e^+e^- \rightarrow b\bar{b}h$ , where center-of-mass-energy of  $e^+e^-$  is 1 TeV and  $m_h = 150$  GeV. Other model parameters are same as Fig. 4.